

Correlation of two particles on a sphere

Gregory S. Ezra and R. Stephen Berry

Department of Chemistry and The James Franck Institute, The University of Chicago, Chicago, Illinois 60637

(Received 18 September 1981)

We consider the correlation of two particles on a sphere interacting via various repulsive forces: a Coulomb repulsion, a Gaussian, and a δ function. This "rigid-bender" picture with Coulomb repulsion provides a schematic model of intrashell angular correlation in doubly excited two-electron atoms. We examine energy levels and reduced densities $\rho(\theta_{12})$ for states corresponding to shells $n_1 = n_2 = 2, 3, 4$. Energy levels for fully converged states fall into remarkable rovibrator patterns, as found in the corresponding three-dimensional case by Kellman and Herrick. The rovibrator nature of the states is directly reflected in plots of $\rho(\theta_{12})$, which reveal both collective rotations and vibrations and even the influence of centrifugal distortion. A minimal basis ($l_{\max} = n - 1$) is inadequate to represent angular correlation in the higher-energy states of each shell. The repulsive Gaussian potential, which is finite at $\theta_{12} = 0$, shows the onset of independent-particle shell-model behavior in higher-energy states. Comparison of the Coulomb case with the delta-function potential exhibits the degree to which kinematics governs wave-function character.

I. INTRODUCTION

The dynamics of electrons in doubly excited states of two-electron atoms is dominated by the interelectronic Coulomb repulsion. For such states, individual particle orbital angular momenta are not at all conserved quantities, and there have been many efforts to find approximate constants of the motion with which to classify the configuration-mixed states.¹⁻¹¹

Recent work¹¹⁻¹⁴ has shed important new light on the nature of doubly excited states. Starting from a group-theoretical point of view, Kellman and Herrick¹¹⁻¹³ organized the manifold of two-electron states resulting from reduction of the direct product of two $O(4)$ irreducible representations [associated with the $O(4)$ degeneracy of hydrogenic atom shells] into larger "multiplets" of states in two complementary ways, so called I and d supermultiplets. When organized in this way, computed energy levels for intrashell states fall into patterns highly suggestive of those associated with the rotation-vibration spectrum of a linear XY_2 triatomic molecule¹⁴ with zero quanta of symmetric and asymmetric stretch vibrations. The manifold of states is truncated due to the finite number of shell states involved. The recognition of supermultiplets extended earlier work in which rotor series had been identified in calculated energy level patterns.¹⁵ Furthermore, Kellman and Herrick were able to demonstrate a 1:1 correspondence between symmetry labels arising from the super-

multiplet scheme and the usual quantum numbers for a bending, rotating linear triatomic.¹⁶ In this way, they fit the calculated spectra quite satisfactorily using molecular term formulas, and derived scaling laws for the effective molecular parameters. Characteristic ratios of rotational to vibrational energies were found to be significantly larger than those for conventional rigid molecules, indicating that the two-electron system in fact behaves as a rather "floppy" XY_2 molecule. The remarkable result is that intrashell doubly excited states appear to exhibit the properties of collective rotation and vibration, at least for low values of nuclear charge. Both phenomena are, of course, well known in molecules and nuclei,^{16,17} but are traditionally unexpected for atomic systems.

The present work is concerned with the further elucidation of these findings and with their general significance for collective motion in few-body systems. We wish to determine to what extent phenomenologically identified rotation-vibration patterns can be related to intrinsic "moleculelike" features of the two-electron wave functions. In particular, is the naive inference that the electrons are localized at about the same distance from the nucleus but on opposite sides with interelectronic angle around 180° really correct? In short, does a doubly excited atom have a shape?

We have already shown by examination of conditional probability densities¹⁸ from accurate Hylleraas-Kinoshita wave functions for He, H^- , and Li^+ that the Kellman-Herrick picture is essen-

tially confirmed for S^e (Ref. 19) and P^o states of the $N=2$ shell.²⁰ Thus, the lowest $^1S^e$ state of He is a "rotor state" corresponding to the ground rotational state with zero quanta of bending vibration; the next-highest $^3P^o$ state is also a rotor state, having one unit of rotational excitation; the $^1P^o$ state corresponds to one quantum of bending vibration, where the bend is, in fact, clearly coupled by Coriolis interactions to "asymmetric-stretch" motion, and the highest $^1S^e$ state is a rotationless state with two quanta of bend. The molecular interpretation of these states is precisely that suggested by Kellman and Herrick. We also note that the intershell "2s 3s" $^3S^e$ states of He and Li^+ are associated with pure "antisymmetric-stretch" motions of a normal vibrational mode, again as expected from the molecular picture.¹⁴

Eventually we would like to extend these detailed analyses of accurate two-electron wave functions to include all the states in a given doubly excited shell. Work along these lines is currently in progress.²¹

The present paper, however, is concerned with a particular aspect of two-electron dynamics, namely, angular correlation. Recognizing that electronic radial wave functions tend to be fairly sharply peaked at characteristic distances corresponding to shell radii, we consider a model problem involving the motion of two particles (electrons) on the surface of a sphere of fixed radius interacting via a Coulomb repulsion. Such a picture with frozen radial motions enables us to study angular correlation in the absence of any interaction with in-out radial correlation, and has been used previously by Herrick as a schematic model for intrashell doubly excited states.²² This model is, however, nothing more than Bunker's "rigid-bender" model for triatomics exhibiting large-amplitude bending motion,²³ so that contact can readily be made with the concepts of molecular spectroscopy.

For two particles on a sphere, we find that calculated energy levels fall into well defined patterns suggestive of collective rotations and vibrations. The main purpose of the present work is to show that, for particles on a sphere at least, the rovibrator nature of the system inferred from calculated energies is directly reflected in the forms of the wave functions themselves. It is interesting to find that superposition of relatively few independent-particle configurations leads to correlated wave functions that are so clearly moleculelike, in which we can readily identify collective rotational and vibrational states and even observe such subtle ef-

fects as centrifugal distortion.

In this paper we proceed as follows: Section II deals with the simple quantum-mechanical calculations involved. The key point here is that, although our straightforward calculations of energy levels and wave functions are all carried out in independent-particle space-fixed coordinates, there is a general and tractable expression for calculating $\rho(\theta_{12})$, the reduced two-particle density, as a function of the interelectronic angle θ_{12} only. It is therefore possible to move into an atom-fixed frame to examine the form of the two-electron density. Energies and reduced densities $\rho(\theta_{12})$ for states corresponding to shells $n_1=n_2=2,3,4$ are presented in Sec. III. While we mainly present fully converged results, the effect of incomplete bases, specifically, minimal or DESB-type with $l \leq N-1$, is examined briefly. As mentioned above, energies for correlated functions fall into remarkable rotation-vibration patterns, just like those found in the three-dimensional case. In Sec. IV we consider two non-Coulombic interparticle interactions, the repulsive δ function and Gaussian potentials. The extremely short-range δ function potential is in a sense the direct opposite of the long-range Coulomb interaction, so that examination of reduced densities in this case shows the extent to which kinematics determines the form of the wave function. At low energies a smooth Gaussian potential confines the particles on opposite sides of the sphere, leading to rotor states with $\theta_{12} \sim \pi$. At slightly higher energies electron density can, however, shift into the region around $\theta_{12} \sim 0$, owing to the finite value of the potential there; this is in contrast to the Coulomb case where the potential is infinite at $\theta_{12}=0$. Our general conclusions are given in Sec. V.

II. CALCULATION OF ENERGY LEVELS, WAVE FUNCTIONS, AND REDUCED DENSITIES

The quantum-mechanical calculations required to obtain energy levels and wave functions for two particles on a sphere are very straightforward. We need to solve the Schrödinger equation

$$\hat{H}\psi = E\psi \quad (1)$$

with two-particle Hamiltonian

$$\hat{H} = -2Z/R + \frac{\vec{1}_1^2}{2R^2} + \frac{\vec{1}_2^2}{2R^2} + \frac{1}{r_{12}} \quad (2)$$

in atomic units, where R is the radius of the sphere

Z is the nuclear charge, \vec{l}_i is the orbital angular momentum vector for electron i and $1/r_{12}$ is the interelectronic Coulomb repulsion. The electron-nucleus Coulomb attraction $-2Z/R$ merely adds a constant term to the energy and may be disregarded. In fact, the only role of the nuclear charge Z in this model problem is to scale the size of the sphere R (see below). The two-electron spatial wave function with total orbital angular momentum quantum numbers j and m is expanded in terms of a coupled single-particle angular momentum basis:

$$\psi_m^j(\hat{r}_1, \hat{r}_2) = \sum_{j_1 j_2} \sum_{m_1 m_2} c_{j_1 j_2 j} Y_{m_1}^{j_1}(\hat{r}_1) \times Y_{m_2}^{j_2}(\hat{r}_2) \langle j_1 m_1 j_2 m_2 | jm \rangle, \quad (3)$$

where antisymmetrization is taken care of by the conditions $c_{j_1 j_2 j} = c_{j_2 j_1 j}$ for a singlet function and $c_{j_1 j_2 j} = -c_{j_2 j_1 j}$ for a triplet, and the parity π is $(-)^{j_1+j_2}$. The electron-electron Coulomb interaction is then expanded in familiar fashion

$$1/r_{12} = 1/R \sum_k C_k(\hat{r}_1) \cdot C_k(\hat{r}_2) \quad (4)$$

and matrix elements evaluated using standard angular momentum techniques.²⁴ All matrix diagonalizations are performed using standard EISPACK routines.

Proceeding in this way we have been able to obtain fully covered energy levels—typically to 7–8 significant figures—for two electrons on spheres of various radii, together with correspondingly converged wave functions. Convergence for all states of interest is usually found at about 10–15 angular configurations, although up to 40 angular configurations have been used as a check in many cases.

The method for calculating the sphere radii R corresponding to particular shells must be explained. In their supermultiplet analysis of doubly excited manifolds,¹³ Kellman and Herrick obtained the dependence of the effective rotational constant on the principle shell quantum number N for He and H^- , viz.,

$$B_e = 0.169N^{-4.38} \text{ He}, \quad (5)$$

$$B_e = 0.058N^{-4.29} \text{ H}^-. \quad (6)$$

We have used these results together with the expression for the rotational constant appropriate for

a rigid linear XY_2 molecule

$$B_e = 1/4R^2 \quad (7)$$

to calculate effective sphere radii for shells with $n_1 = n_2 = 2, 3, 4, 5$ for He and H^- . The resulting values of R are given in Table I. Although this simple prescription for the effective sphere radii yields values that are somewhat larger than expected from the positions of maxima in typical radial distribution functions, the qualitative features of the results described in the next section are in fact insensitive to the precise choice of R . (It is well known from nuclear physics that the moment of inertia problem, i.e., the problem of the interpretation of effective rotational constants derived from observed or computed collective rotation spectra, in general presents many difficulties¹⁷).

Having obtained accurate wave functions for two particles on a sphere whose radius corresponds to a particular doubly excited intrashell manifold for either He or H^- , we can calculate the reduced two-electron density as a function of the interelectronic angle θ_{12} . The function $\rho(\theta_{12})$ contains all essential information on interparticle correlation on the sphere, since it excludes irrelevant details concerning the rotational wave function of the system, the latter being determined essentially by rotational symmetry alone.²⁵ A general expression for $\rho^{(j)}(\theta_{12})$ for an arbitrary two-electron wave function having total angular momentum j and expressed in terms of single-particle coordinates is derived as follows:

(i) Form the rotational-invariant two-electron density by summing over the magnetic quantum number m :

$$\rho^{(j)}(\hat{r}_1, \hat{r}_2) \equiv \frac{1}{(2j+1)} \sum_{m=-j}^j \psi_{jm}^* \psi_{jm}. \quad (8)$$

(ii) Recouple the single-particle angular momenta to give a rotationally invariant expression for $\rho^{(j)}(\hat{r}_1, \hat{r}_2)$ in terms of Legendre polynomials $P_k(\cos\theta_{12})$.

TABLE I. Values of sphere radius R in atomic units for shells $N = 2, 3, 4, 5$ and nuclear charges $Z = 1, 2$ (calculated from Ref. 13).

	He $Z = 2$	H^- $Z = 1$
$N = 2$	5.6	9.2
3	13.7	22.0
4	25.8	40.9
5	42.0	66.1

(iii) Integrate directly over the Euler angles describing the orientation of the electron-nucleus-electron triangle in space. Since the Jacobian for the transformation from independent-particle angular coordinates to Euler angles describing the orientation of the atom-fixed frame together with

θ_{12} is $+1$ with natural weight functions,²⁶ this step simply involves multiplication by the Euler angle volume $8\pi^2$.

We thereby obtain an explicit expression for the reduced density $\rho^{(j)}(\theta_{12})$ in terms of the coefficients $c_{j_1 j_2 j}$:

$$\rho^{(j)}(\theta_{12}) = \sum_{\substack{j_1 j'_1 \\ j_2 j'_2}} c_{j'_1 j'_2 j}^* c_{j_1 j_2 j} \frac{1}{2} [(2j_1 + 1)(2j'_1 + 1)(2j_2 + 1)(2j'_2 + 1)]^{1/2} \\ \times \sum_k (-)^{j-k} (2k+1) \begin{pmatrix} j_1 & j'_1 & k \\ 0 & 0 & 0 \end{pmatrix} \begin{pmatrix} j_2 & j'_2 & k \\ 0 & 0 & 0 \end{pmatrix} \begin{pmatrix} j_1 & k & j'_1 \\ j'_2 & j & j_2 \end{pmatrix} P_k(\cos\theta_{12}). \quad (9)$$

There are several points to be noted concerning this result. First of all, it is an explicit and tractable expression involving a natural expansion of the reduced *density* in terms of Legendre polynomials. The sum over the extra variable k is finite, terminating at $k_{\max} = \min(j_1 + j'_1, j_2 + j'_2)$. The expression (9) is much more convenient than that given previously by Rhemus *et al.*,¹⁸ which involved an integral over a function of both old and new coordinates. The reduced density $\rho^{(j)}(\theta_{12})$ is correctly normalized, as is easily verified

$$\int_{+1}^{-1} \rho^{(j)}(\theta_{12}) d(\cos\theta_{12}) = \sum_{j_1 j_2} |c_{j_1 j_2 j}|^2. \quad (10)$$

Also, the expression for $\rho^{(j)}(\theta_{12})$ is identical with the expectation value of the angular delta function $\delta(\cos\theta_{12} - \cos\theta'_{12})$, which is just the two-particle angular density matrix

$$\rho^{(j)}(\theta_{12}) = \sum_{\substack{j_1 j'_1 \\ j_2 j'_2}} c_{j'_1 j'_2 j}^* c_{j_1 j_2 j} \sum_k \frac{(2k+1)}{2} \langle j'_1 j'_2 j | | C_k(1) \cdot C_k(2) | | j_1 j_2 j \rangle P_k(\cos\theta_{12}). \quad (11)$$

This formula has recently been used by Warner *et al.*²⁷ Finally, the value of $\rho^{(j)}(\theta_{12})$ at $\theta_{12}=0$ is given by

$$\rho^{(j)}(\theta_{12}=0) = \sum_{\substack{j_1 j'_1 \\ j_2 j'_2}} c_{j'_1 j'_2 j}^* c_{j_1 j_2 j} \frac{1}{2} [(2j_1 + 1)(2j'_1 + 1)(2j_2 + 1)(2j'_2 + 1)]^{1/2} \\ \times \begin{pmatrix} j_1 & j_2 & j \\ 0 & 0 & 0 \end{pmatrix} \begin{pmatrix} j'_1 & j'_2 & j \\ 0 & 0 & 0 \end{pmatrix}, \quad (12)$$

which is (twice) the "pairing density" defined by Herrick.²²

In the next section energy levels and reduced densities obtained by the methods just described are examined in some detail.

III. COULOMB POTENTIAL

Figure 1 shows fully converged calculated energies of 19 states for two electrons on a sphere of radius 13.7 bohr, corresponding to the states of the He $N=3$ doubly excited shell. The first thing to

be noted is that the energy level pattern is strikingly similar to those calculated for the three-dimensional case by Herrick and Kellman,^{13,14} and clearly has the appearance of a fragment of the rotation-vibration manifold of a linear triatomic molecule with a low ratio of bending to rotation frequency. There is, however, one important difference between the level patterns for converged states of particles on a sphere and electrons in an atom. Thus, in the real atomic case the so-called $T(l)$ doubling has *opposite sign* to that for electrons on a sphere or linear molecules. The significance of this reversal is discussed below. Each state can

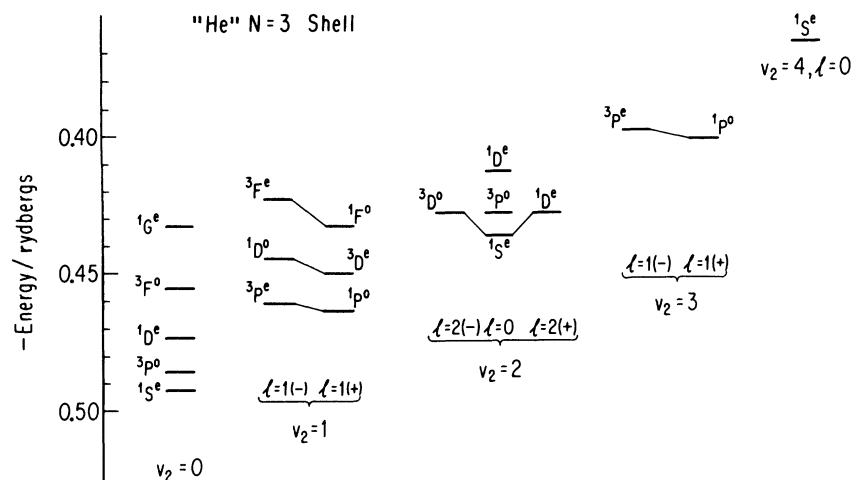


FIG. 1. Calculated energy levels for two particles on a sphere of radius 13.7 bohr interacting via a Coulomb repulsion. The 19 states shown correspond to the He $N=3$ doubly excited shell, and are arranged according to the rotation-vibration pattern. Assigned molecular quantum numbers are also shown (see text).

be assigned a set of molecular quantum numbers based upon its position in the calculated rotation-vibration manifold. These quantum numbers are v_2 , the number of quanta of bending vibration, l , the projection of the vibrational angular momentum due to the degenerate bending mode along the molecular axis, and J , the total angular momentum. The following hierarchical relations hold:

$$v_2=0, 1, 2, \dots, \quad (13a)$$

$$l=v_2, v_2-2, v_2-4, \dots, 1 \text{ or } 0, \quad (13b)$$

$$J=l, l+1, \dots \quad (13c)$$

For every state the parity and permutational symmetries given in the term symbol agree with those calculated from the associated molecular quantum numbers.^{16,28}

According to the molecular picture, the five states $1S^e$, $3P^o$, $1D^e$, $3F^o$, and $1G^e$ on the left-hand side of Fig. 1 form a rotor series based on the vibrationless ground state. The calculated energy levels for these states are indeed very closely fitted by the rigid-rotor expression $E_J = BJ(J+1)$; the

TABLE II. Rotational constants B for $N=2, 3, 4$ shells of "He" ($B/10^{-3}$ Ry). Column A: Fitted to "observed" levels. Column B: Rigid rotor value $1/4R^2$ a.u.

$B/10^{-3}$ Ry	A	B
$N=2$	20.0	15.9
3	3.0	2.66
4	0.82	0.71

derived value of the rotational constant B is 3×10^{-3} Ry, which is in good agreement with a rigid-rotor value of $1/4R^2$ atomic units $\sim 2.7 \times 10^{-3}$ Ry (cf. Table II).

It can therefore be inferred that correlation of electrons on the sphere results in localization of the particles around $\theta_{12} \sim \pi$, and that collective rotation of the linear configuration of particles can then occur.

Bending vibration levels are also clearly identifiable in Fig. 1. For example, the three nearly evenly spaced $1S^e$ states shown correspond (left to right) to 0, 2, and 4 quanta of bending vibration, respectively. In addition, closely spaced doublets such as $3P^e/1P^o$, $3D^o/1D^e$ are assigned to vibrational levels with nonzero values of l . Thus, the sequence of doublets $3P^e/1P^o$, $1D^o/3D^e$, and $3F^e/1F^o$ form a rotor series with vibrational angular momentum $l=1$. In the absence of any interaction between bending and rotational motion, the l (or T) (Ref. 12) doublets would be degenerate; in fact, calculated centrifugal splittings increase with increasing angular momentum J , as expected.¹⁶ Note that left- (right-) hand partner states are $-$ ($+$) states analogous to (\pm) lambda-doublet eigenstates in diatomic molecules.²⁹

Rotational constants and bending frequencies obtained from calculated energy levels are given in Tables II and III, respectively, for the $N=2, 3, 4, 5$ shells of "helium". The fitted values of vibrational frequencies are in good agreement with those calculated from a harmonic approximation to the interparticle Coulomb potential obtained by expand-

TABLE III. Vibrational frequencies for $N=3,4,5$ shells of "He" ($/10^{-2}$ Ry). Column A: Values obtained from calculated spacings of levels with fully converged calculations. Column B: Values obtained from the harmonic term in the expansion of potential about the linear configuration. Column C: Values obtained from the shape of the wave function.

	A	B	C
$N=3$	19.0	19.7	18.9
4	7.45	7.57	7.52
5	3.62	3.67	3.58

ing about the linear configuration.¹⁴ Higher-order rotation-vibration constants have not been fitted to these levels.

We therefore conclude from our examination of calculated energy levels that, in addition to undergoing overall collective rotation, two electrons on a sphere execute well-defined bending vibrations about the linear configuration, and that there is significant but not overwhelming vibration-rotation interaction.

We now turn to the calculated densities $\rho(\theta_{12})$ in order to determine whether or not the inferences drawn above concerning localization are in fact supported by the forms of the electron distributions themselves. First recall that densities associated with pure linear molecule wave functions are well known. If the state has vibrational quantum numbers v_2 and l , and the bending coordinate is $\beta = (\pi - \theta_{12})/2$, the density ρ is the function³⁰

$$\rho = N_{v_2, l}^2 e^{-\xi^2} \xi^{2l} [L_n^l(\xi^2)]^2, \quad (14)$$

where $n = (v_2 - l)/2$ is the number of nodes in the angular wave function, $\xi = (k\mu)^{1/4} \beta$ is a scaled bending coordinate, $\mu = 2R^2$ is the reduced mass for bending, the harmonic approximation to the bending potential is given by $V \sim 1/2k\beta^2$, and $N_{v_2, l}$ is a normalization constant.

Figure 2 shows density profiles $\rho(\theta_{12})$ for all the $N=3$ shell states given in Fig. 1, calculated from the corresponding fully converged wave functions. The quantity actually plotted is ρ/ρ_{\max} vs θ_{12} , where ρ_{\max} is the maximum value of the density in the interval 0 to π , so that all plots are normalized to unity.

The plots in Fig. 2 display many significant and striking regularities. First of all, we see that the five states provisionally assigned to a rotor series based on the vibrationless ground state have virtually indistinguishable (scaled) profiles $\rho(\theta_{12})$, which

are to very good approximation Gaussian in shape. This result reveals the essential feature of collective rotation, which is that the set of states forming a collective rotor series have an internal shape which is little altered by addition of rotational angular momentum to the system.³¹ In fact, there are slight but systematic variations of the density profiles with increasing angular momentum, due to centrifugal distortion (see below). From the half-width of the ground state $^1S^e$ Gaussian profile it is possible to calculate an effective vibrational frequency in good agreement with the "observed" and harmonic approximation value (Table III).

In three doublets $^3P^1/1P^0$, $^1D^0/3D^e$, and $^3F^e/1F^0$ assigned to $v_2=1$ form a particularly interesting set of states. We see that the density profiles $\rho(\theta_{12})$ for near degenerate l -doublet partner states are identical; it should be emphasized that partner states have distinct global symmetries and spins, so that the corresponding wave functions and ρ 's are obtained from completely independent blocks of the Hamiltonian. The densities themselves have precisely the form expected from (14) for states with vibrational quantum numbers $v_2=1$ and $l=1$, confirming the original assignment. It can also be seen that there is relatively little centrifugal distortion of the $v_2=1$ profiles, at least up to $J=3$ (F states).

The nodal structure of the reduced two-electron density is of some importance. Since the Coulomb repulsive potential rises to infinity at $\theta_{12}=0$, all wave functions are expected to vanish at this point unless constrained to do otherwise. In addition, for some space and spin symmetries the two-electron wave function and hence ρ must necessarily have a node at $\theta_{12}=\pi$. Thus, when $\theta_{12}=\pi(\hat{r}_1 = -\hat{r}_2)$ the following two operations must have an identical effect on the wave function:

(i) Interchange of particle coordinates

$$\hat{r}_1 \leftrightarrow \hat{r}_2 = -\hat{r}_1 .$$

(ii) Inversion

$$\hat{r}_1 \rightarrow -\hat{r}_1, \hat{r}_2 \rightarrow -\hat{r}_2 .$$

For the wave function to be nonzero at $\theta_{12}=\pi$ we must therefore have $(-)^{j_1+j_2} = +1$ (singlet), $(-)^{j_1+j_2} = -1$ (triplet), so that the following states rigorously have nodes at $\theta_{12}=\pi$: triplet even and singlet odd. All the $v_2=1$ manifold of states are therefore constrained to have a node at $\theta_{12}=\pi$, irrespective of the exact degree of resemblance to $2-d$ oscillator functions. The two-electron wave function also vanishes identically at $\theta_{12}=\pi$ or 0 if it is

in accord with the discussion of T doubling given in Ref. 14.

It is therefore important to note an essential difference between electron correlation in the real atom and that found in the model system of two particles on a sphere. By including sufficiently many angular configurations for the two particles on a sphere, it is possible to obtain enough angular correlation so that $\rho(\theta_{12}=0) \sim 0$ for singlet ρ -doublet states without Class I nodes, e.g., $^1P^o$, and the system behaves like an asymmetric top. Presumably in-out radial correlations prevent a similar degree of angular localization in corresponding states in the atomic case. These results imply that, using a smaller angular basis for particles on the sphere, it should be possible to reverse the sign of the l doubling for certain pairs of states. This is indeed the case. The splitting of the upper $^3P^e/{}^1P^o$ pair shown in Fig. 6 (see below) is opposite in sign to that of the lower pair; the upper pair exhibits the atomic ordering and has appreciable density around $\theta_{12}=0$ in the ${}^1P^o$ state, whereas the lower states exhibit the molecular ordering and has $\rho(\theta_{12}) \sim 0$ around $\theta_{12}=0$ for both states.

The three rotor states ${}^1S^e$, ${}^3P^o$, and ${}^1D^e$ assigned the vibrational quantum numbers $v_2=2$, $l=0$ have densities qualitatively just as expected from (14) for two quanta of bend, with the quantitative difference that the actual profiles do not fall off quite as rapidly as the pure molecular wave functions for large values of $\beta=(\pi-\theta_{12})/2$. The two partner states ${}^3D^o/{}^1D^e$ corresponding to the $v_2=2$, $l=2$ pair illustrate the points made above concerning nodal structure. Thus, the ${}^3D^o$ state is constrained to have a Class I node at $\theta_{12}=\pi$, and so has the qualitative shape given by (14). However, the ${}^1D^e$ partner state has no such constraint, and can have finite electron density at $\theta_{12}=\pi$ without violating any symmetry requirement (recall that ${}^1D^e$ corresponds to the (+) partner state of the l doublet). A buildup of density at $\theta_{12}=0$ can be considered a result of mixing of a pure $v_2=2$, $l=2$ molecular wave function with the nearest ${}^1D^e$ level ($v_2=2$, $l=0$). Because the energy of the ${}^1D^e(v_2=2, l=0)$ is higher than that with $l=2$, this mixing leads to lowering of the energy of the $l=2(+){}^1D^e$ state with respect to its partner ${}^3D^o$. We stress that the bump at $\theta_{12}=0$ for the ${}^1D^e$ state is not an artifact resulting from use of too small a basis. Rather, it persists and actually increases with the size of basis until convergence is attained. This mixing of "bending" angular momentum of the $l=2$ state and "rigid" rotation of the $l=0$

state is analogous to Λ doubling in linear molecules. The effect is even more pronounced in the plots of ρ for the $N=4$ shell (see below).

Moving on to the two $v_2=3$, $l=1$, ${}^3P^e/{}^1P^o$ states, we find once again that the calculated reduced densities are remarkably similar and of precisely the form expected from the assigned molecular quantum numbers. There is no nearby rotor state to contribute to Λ doubling for this pair, so they remain almost degenerate, with identical wave functions. Finally, the highest energy ${}^1S^e$ state has a density profile appropriate for a state with 4 quanta of bending vibration.

As mentioned above, the wave functions exhibit the effects of centrifugal distortion. In Fig. 3(a) we superimpose the five reduced densities for the $v_2=0$ rotor series of the $N=3$ shell. It can be seen that there is a progressive narrowing of the Gaussian profiles with increasing angular momentum, due to centrifugal distortion. In classical terms, centrifugal forces resulting from overall rotation have a tendency to push electrons toward the linear configuration, and this effect is manifest in quantum mechanics as a narrowing of the angular distributions around $\theta_{12}=\pi$. Figure 3(b) shows the corresponding effect in the $v_2=2$ rotor series.

Our results on both energy levels and wave functions for the " $N=3$ shell" of two particles on a sphere show that correlation due to Coulomb repulsion induces a remarkable degree of collective, moleculelike behavior. It seems entirely plausible that such molecular behavior may persist in doubly excited states of real two-electron atoms when radial motions come into play, as suggested by the work of Herrick and Kellman.

We now describe much more briefly results for some other "shells." In Fig. 4 we show reduced densities for the six states corresponding to the He $N=2$ shell ($R=5.6$ bohr). Whereas the states of the $N=3$ shell were displayed in Fig. 2 so as to bring out the rotation-vibration structure as clearly as possible, the states in Fig. 4 are arranged slightly differently to form so-called d supermultiplets.¹² All states in a given d supermultiplet have the same number n_2 of nodes (or near nodes, since d is not a rigorously good quantum number) in the bending wave function between $\theta_{12}=0$ and π . The relation between d and n_2 is

$$n_2 = N - d - 1 = (v_2 - l)/2, \quad (15a)$$

$$d = 0, 1, \dots, N - 1, \quad (15b)$$

where N is the shell principal quantum number, so

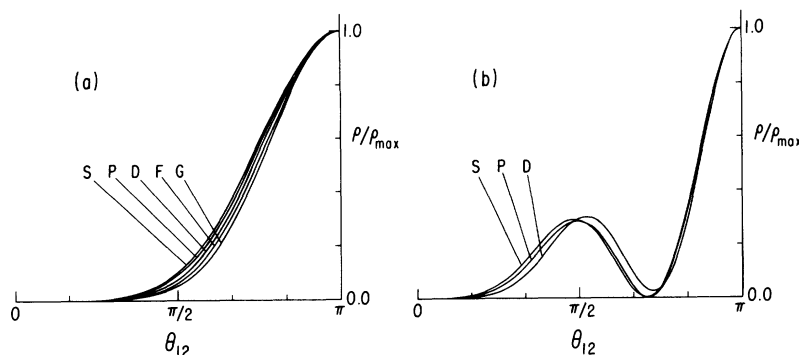


FIG. 3. Centrifugal distortion in the "He $N=3$ shell." In (a) we superimpose density profiles for $v_2=0$ rotor series, while in (b) density profiles for the $v_2=2$ rotor series are superimposed.

that d supermultiplets are made up of states having constant values of the difference $v_2 - l$ (which may be interpreted as the degree of excitation in the bending mode¹³). The states in a given d supermultiplet are arranged symmetrically around a central column of states with $l=0$, with l (and therefore v_2) increasing by one per step to the left or right, and total angular momentum J increasing vertically. These points are illustrated in Fig. 4, which shows the two d supermultiplets associated with the He $N=2$ shell. The $d=1$ supermultiplet contains five states with no nodes in the bending wave functions ($n_2=0$): these are the rotor series $^1S^e$, $^3P^o$, and $^1D^e$ with $v_2=0$ $l=0$, and the $v_2=1$ $l=1$ doublet $^3P^e/{}^1P^o$. The $d=0$ supermultiplet consists of one state, $^1S^e$ with $v_2=2$. The moleculelike character of all the states is evident from Fig. 4; note particularly the similarity between density profiles for partner states $^3P^e$ and $^1P^o$. Following Herrick and Kellman, $+(-)$ states appear on the right- (left-) hand side of a d supermultiplet.

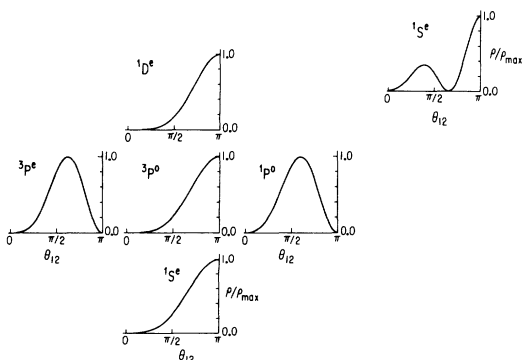


FIG. 4. Reduced two-electron densities for the "He $N=2$ shell" (sphere of radius 5.6 bohr). The states are arranged in so-called d supermultiplets.

Figure 5(a) shows the $d=3(n_2=0)$ supermultiplet of the "He $N=4$ shell" ($R=25.8$ a.u.). The notable features are by now familiar:

- (i) a well-defined central ($v_2=0$) collective rotor series, in which the states have Gaussian profiles;
 - (ii) well-defined l doublets associated with degenerate collective bends, with reduced densities qualitatively similar to those given by (14); for example, the ξ^l factor in (14) implies a slower rise of ρ away from $\xi=0$, $\theta_{12}=\pi$ with increasing l : just such a trend can be observed in the states $^3F^e[l=1(-)]$, $^1F^e[l=2(-)]$, and $^3F^e[l=3(-)]$;
 - (iii) pronounced centrifugal mixing leading to a buildup of electron density at $\theta_{12}=\pi$ for states where this is allowed by symmetry [for example, the $l=2(+)$ rotor series $^1D^e$, $^3F^o$, and $^1G^e$].
- In Fig. 5(b) we show the remaining states of the $N=4$ shell, arranged into d supermultiplets. The molecular character of the wave functions is apparent throughout the whole $N=4$ intrashell manifold.

In the remainder of this section we examine very briefly the effect of an inadequate basis upon the calculated reduced densities. It is of particular interest to make a comparison between fully converged wave functions and those constructed using a minimal angular basis, i.e., one in which the maximum value of the single-particle angular momentum l is $N-1$ for a given shell. This latter case is important since $O(4)$ -based theories of correlation in doubly excited intrashell states use a direct product basis of hydrogenic functions where the above restriction on l holds. The question is, then, how well does a minimal basis represent angular correlation?

In Fig. 6 we show reduced densities for the He $N=3$ shell calculated from wave functions obtained with a minimal angular basis. Figure 6

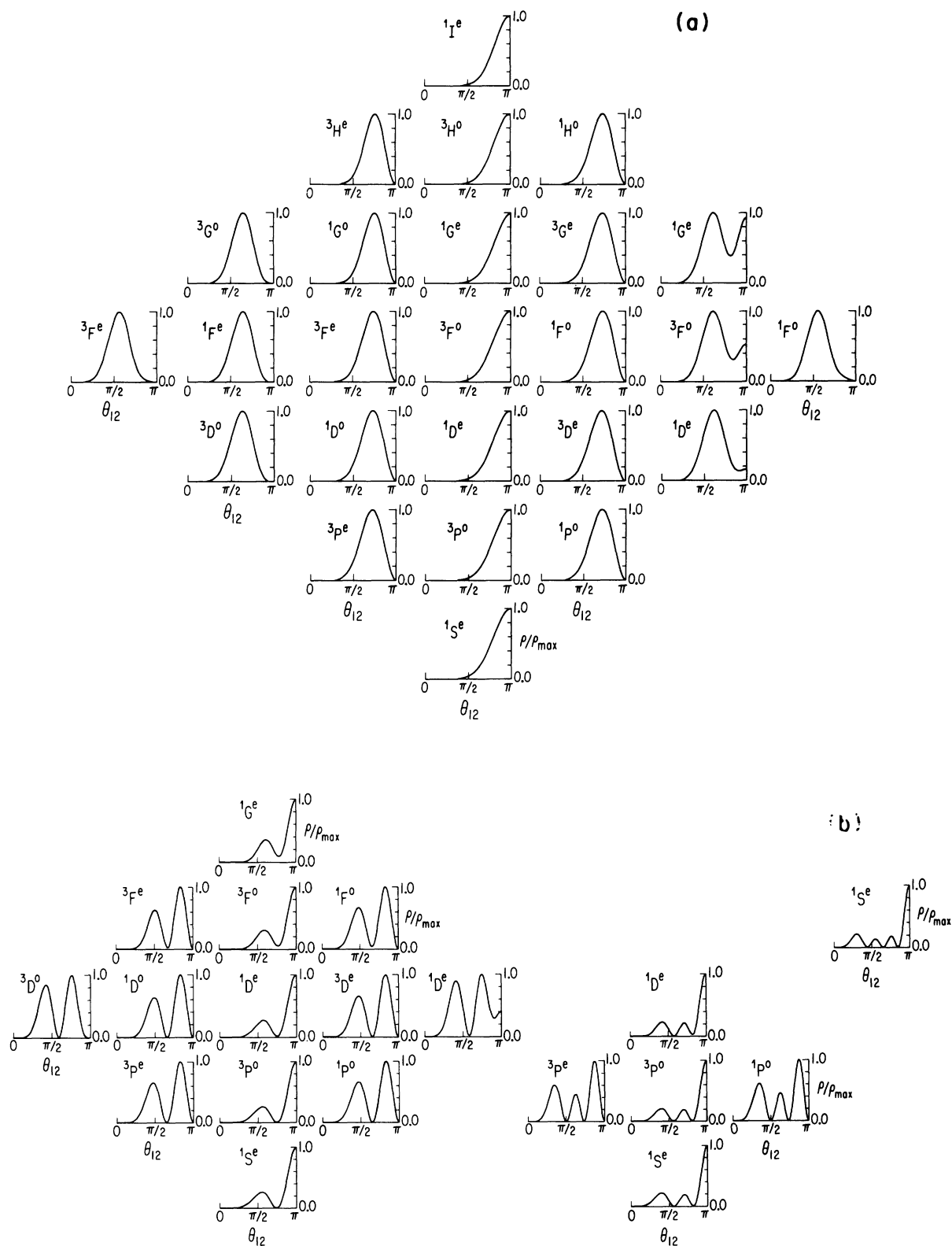


FIG. 5. Reduced two-electron densities for the "He $N=4$ shell" (sphere of radius 25.8 bohr). (a) shows the $d=3$ supermultiplet, while (b) shows the $d=2, 1, 0$ supermultiplets.

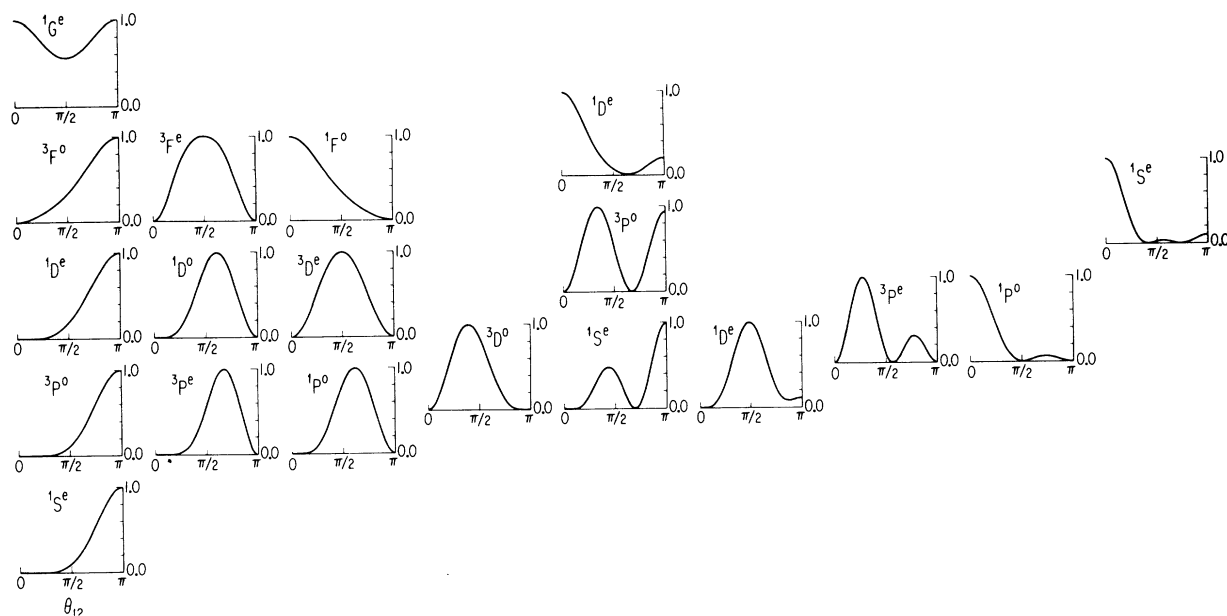


FIG. 6. The effects of an inadequate angular basis. We show reduced two-electron densities $\rho(\theta_{12})$ calculated for the “He $N=3$ shell” using a minimal angular basis ($l \leq 2$).

must be compared directly with Fig. 2. Several qualitative features are immediately obvious. Thus, there are states of low energy whose wave functions (and energies) are well described using a minimal basis, e.g., $1S^e(v_2=0)$, $1S^e(v_2=2)$, $3P^e/1P^o(v_2=1, l=1)$. However, with increasing energy the ability of the basis to give the correct trends found with fully converged wave functions is limited. For example, we note that the density profiles in the $v_2=0$ rotor series appear to spread out with increasing angular momentum rather than contract, as they do with converged functions. Similarly, the reduced densities for partner states $1D^o/3D^e(v_2=1, l=1)$ are no longer identical with those derived from a minimal basis. Finally, there are several states at high energies for which use of a minimal basis leads to qualitatively incorrect forms of the reduced density. Examples are the $1G^e(v_2=0)$, $1F^o(v_2=1, l=1)$, $1D^e(v_2=2, l=0)$, $1P^o(v_2=3, l=1)$, and $1S^e(v_2=4)$ states. In all these cases there is an apparent localization of electron density at $\theta_{12}=0$, which is characteristic of so-called *antirrotor* states. Such antirrotor character is here clearly spurious, being a consequence of the orthogonality constraints imposed by use of too small an angular basis. An apparent localization around $\theta_{12}=0$ was also noted by Brickstock and Pople³² for single-configuration $1P^o$ two-electron wave functions.

Similar results are found when using minimal

angular bases for other shells. In general we find that, for a given shell, it is necessary to include single-particle angular momenta up to a value of N in the basis to obtain correctly the gross trends in the reduced density, whereas to obtain subtle features such as centrifugal contraction we require single-particle angular momenta up to $N+1$.

The implications for calculations of real two-electron atoms are of some interest, since our results suggest that use of a DESB-type basis^{7,18} leads to a qualitatively incorrect representation of angular correlation in higher states of doubly excited shells. This conclusion is borne out by some previous calculations on the “ $2p^{2\prime}$ ” $1S^e$ state of He^{**} , where the “antirrotor” nature of the state found using a DESB basis changes to rotorlike with a more accurate Hylleraas-Kinoshita wave function (Ref. 19), compare especially Figs. 9(e) and 10(b).

IV. NON-COULOMBIC POTENTIALS

In this section we examine energy levels and reduced densities for two particles on a sphere interacting through non-Coulombic potentials. Comparison is made with the results of the previous section.

Consider first two “electrons” on a sphere interacting via a Gaussian potential of the form shown in Fig. 7. This potential is smooth and at-

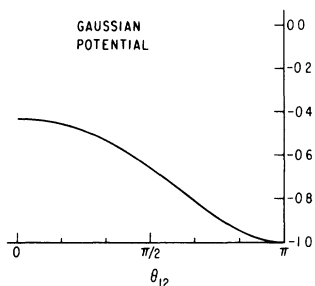


FIG. 7. The Gaussian potential used in our calculations. Note that this potential forms a smooth well at the linear configuration, i.e., $\theta_{12} = \pi$.

tractive at $\theta_{12} = \pi$, and has the expansion

$$V(R, \theta_{12}) = S \exp[-2R^2(1 + \cos\theta_{12})/W^2], \quad (16a)$$

$$= \sum_k i^{-k} (-)^k (2k+1) e^{-2R^2/W^2} \times j_k(2iR^2/W^2) P_k(\cos\theta_{12}), \quad (16b)$$

where S is a strength parameter and W is the width of the Gaussian. The Gaussian mimics short-range atom-atom potentials around $\theta_{12} = \pi$ but corresponds to penetrable particles around $\theta_{12} = 0$. We have found that some care is necessary when using the expansion (16b), since it is apparently asymptotic; typically we retain only the first 8–10 terms.

Figure 8 shows fully converged energy levels for the states of the “ $N=3$ shell.” Parameters for the

Gaussian potential are $R = 13.7$ bohr, $S = -0.05$ a.u., and $W = 30$ bohr. This combination of strength and width parameters gives a reduced density for the lowest $^1S^e$ state almost identical with that for the Coulomb potential (see below). The energy levels in Fig. 8 should be compared with the corresponding levels for the Coulomb case in Fig. 1. It can be seen that, although the levels of Fig. 8 still fall into a recognizable rotation-vibration pattern, there are marked differences between the Gaussian levels and the vibrator rotator. Despite the strong resemblance of the main ($\nu_2 = 0$) rotor series for the Gaussian potential to that for the Coulomb case, implying a similar degree of localization of the particles, the three “ $\nu_2 = 2$ ” states $^1S^e$, $^3P^o$, and $^1D^e$ no longer form a well-defined rotor series. Centrifugal splittings also increase rapidly with energy, distorting the rotation-vibration pattern. Thus, the splitting between the $\nu_3 = 3$, $l = 1$ partner states $^3P^e$ and $^1P^o$ is of the same order as a bending vibrational spacing.

All this implies that the molecular picture is on the point of breaking down for the higher energy states of the “ $N=3$ shell” with a Gaussian potential, and this conclusion is confirmed by examination of the corresponding reduced densities shown in Fig. 9. The $\nu_2 = 0$ rotor series bending wave functions are very similar to those for the Coulomb case; indeed, as mentioned above, the particular Gaussian potential parameters used here were chosen to make the lowest $^1S^e$ profiles as similar as possible. Moving to the $\nu_2 = 1$ manifold a major

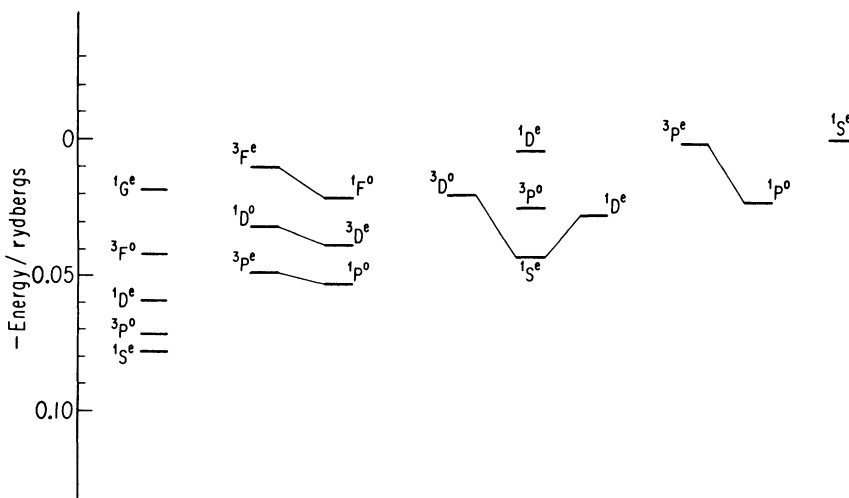


FIG. 8. Calculated energy levels for two particles on a sphere interacting via the Gaussian potential of Fig. 7, with $R = 13.7$, $S = -0.05$, and $W = 30$. The 19 states shown correspond to the “He $N=3$ shell” shown in Fig. 1. Levels are arranged to show the rotation-vibration pattern.

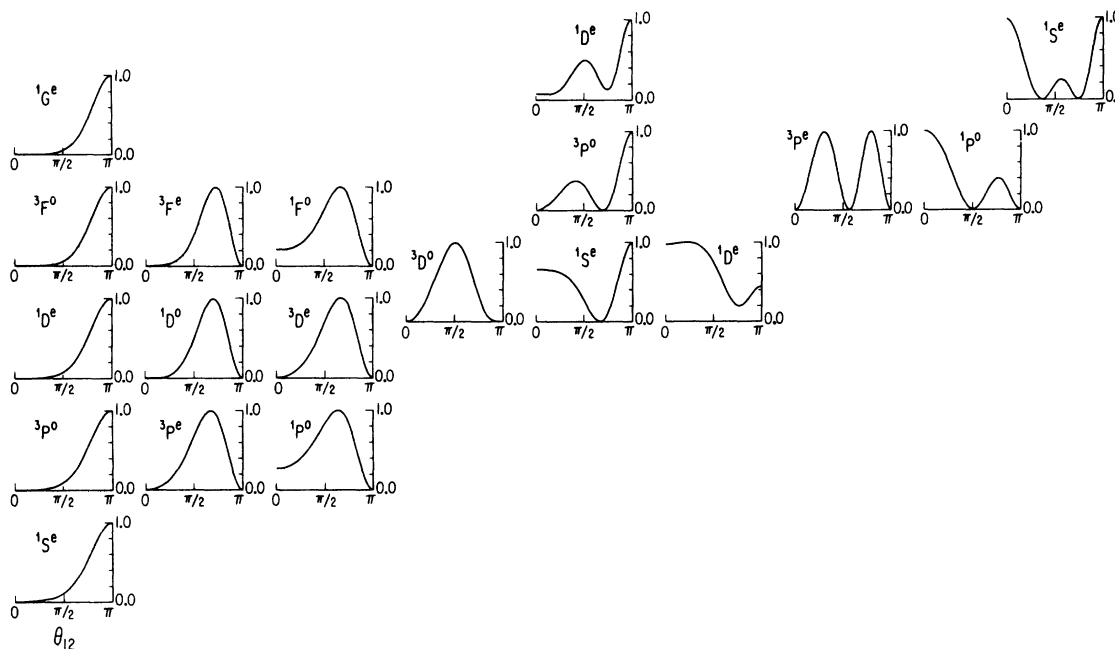


FIG. 9. Reduced two-electron densities $\rho(\theta_{12})$ calculated for the states shown in Fig. 8.

difference becomes apparent. For, due to the finite value of the Gaussian potential (16) at $\theta_{12}=0$, the $1F^o$ and $1P^o$ states are able to build up density at $\theta_{12}=0$, leading to qualitative differences between the wave functions for l -doublet partners. Such a delocalization of the particles away from $\theta_{12}=\pi$ is associated with large centrifugal splittings; witness the gross disparities in the density profiles for the “ $v_2=2$ ”, $3D^o/1D^e$, and “ $v_2=3$ ” $3P^e/1P^o$ pairs. The $v_2=2$ $1S^e$ function is also distorted from the ideal molecular shape; presumably centrifugal forces serve to keep the $1D^e$ more localized around $\theta_{12}\sim\pi$ (the $3P^o$ must of course have a node at $\theta_{12}=0$ due to the Pauli principle). Note that the “ $v_2=4$ ” $1S^e$ state is very nearly symmetrical about $\theta_{12}=\pi/2$, showing that the transition from collective to single-particle dynamics is almost complete with this state (pure angular configurations for $1S^e$ state are characteristically symmetric about $\theta_{12}=\pi/2$).

We are therefore able to observe the onset of independent-particle shell-model behavior in a smooth Gaussian potential of the form shown in Fig. 7. For sufficiently high kinetic energies, the potential can no longer confine the particles around $\theta_{12}\sim\pi$, so that collective molecular behavior breaks down. We have found a similar transition between collective rotations and vibra-

tions and independent-particle dynamics in the motion of two particles moving on concentric spheres of different radii interacting via a Coulomb potential. Increasing the ratio of the radii of the two spheres leads smoothly from semirigid bending vibrations to hindered rotations of one particle around a central core.

Finally, we consider two particles interacting via a delta-function repulsive potential. Figure 10 shows densities $\rho(\theta_{12})$ calculated for six states on a sphere of radius 5.6 bohr, corresponding to the “He $N=2$ shell”, with a delta-function repulsion of unit strength. Figure 10 is to be compared with Fig. 4. Our calculations show directly that the triplet states $3P^e$ and $3P^o$ have pure angular configuration wave functions. This is expected, since, having a node at $\theta_{12}=0$, triplet functions cannot feel the delta-function interaction. Densities for the singlet $1S^e$, $1P^o$, and $1D^e$ states exhibit spurious oscillatory structure due to incomplete convergence, despite the use of a relatively large ($l_{\max}=15-20$) angular basis. Although calculated energy levels by no means form a molecular rotation-vibration pattern, there is nevertheless a certain family resemblance between the two sets of states in Figs. 4 and 10, illustrated by the arrangement of levels into d supermultiplets. Since we

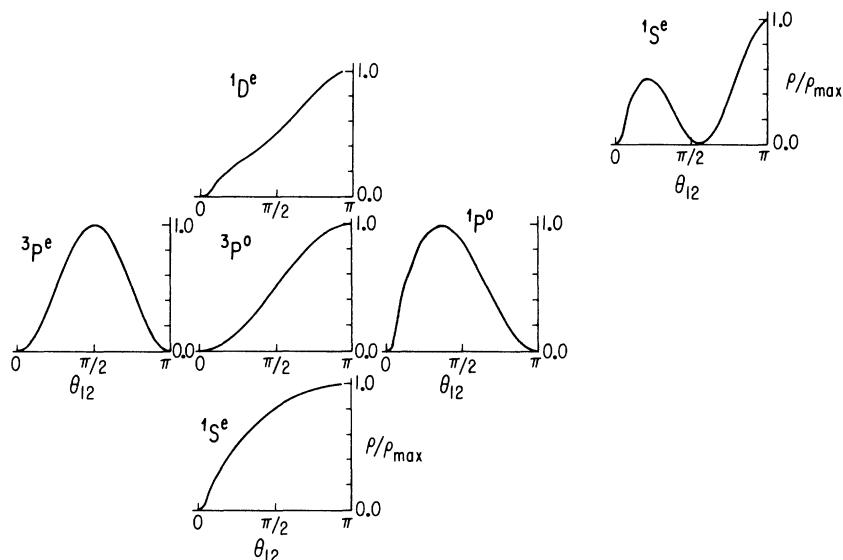


FIG. 10. Reduced two-electron densities $\rho(\theta_{12})$ for two particles on a sphere of radius 5.6 bohr interacting via a delta-function repulsion of unit strength. The six states shown correspond to those of the "He $N=2$ " shell shown in Fig. 4.

have compared states for potentials having completely opposite characteristics (long-range Coulomb versus ultra-short-range delta function), we conclude that kinematics and symmetry constraints are important in determining the form of the wave function.

V. CONCLUSIONS

Several interesting results have emerged from our analysis of the model problem of two particles moving on the surface of a sphere of fixed radius.

First of all, for the Coulomb case, it is remarkable the extent to which purely phenomenological assignments of molecular quantum numbers based on computed energy levels are confirmed by detailed examination of the reduced densities $\rho(\theta_{12})$. The dominant feature in all the states studied is a marked angular correlation and localization of the particles around $\theta_{12} \sim \pi$. This leads to the possibility of collective moleculelike behavior with well-defined separation of rotation and vibration. Antirrotor character only appears as a result of an inadequate angular basis.

For a softer Gaussian interparticle potential, localization only occurs at the lowest energies. At higher energies we observe a transition to inde-

pendent-particle shell-model dynamics, signaled both by gross distortions in the rotation-vibration energy-level pattern and by pure angular configuration character of corresponding wave functions. Such a transition is also observed for the motion of two particles on concentric spheres of different radii, as the radius of one sphere is made much larger than the other.²¹ It is also appropriate to mention here the work of Wyatt and collaborators,³³ who have studied a similar transition between semirigid bending and hindered rotor dynamics in a different context (definition of channel functions for reactive scattering calculations). The possibility of observing such a phenomenon in highly excited local-mode states of small molecules is very intriguing.

Finally, examination of wave functions for states of the repulsive delta-function potential shows that kinematics and symmetry requirements have a substantial part to play in shaping the wave function.

The significance of our work for the elucidation of Kellman and Herrick's phenomenological identification of rotation-vibration patterns in calculated levels of real doubly excited atoms is clear. Since the moleculelike character of states for particles on a sphere with Coulomb interaction is so pronounced, it is reasonable to expect some of this collectivity to carry over into the full three-

dimensional dynamics. Indeed, we have already shown that the $^1S^e$ and $^{1,3}P^o$ doubly excited states of the He $N=2$ shell have significant molecular character.²⁰ However, in-out radial motions will tend to reduce the extent of angular correlation in a given state, while high values of the total angular momentum will increase coupling of "vibrations" with overall rotations. It has also been found that there is a significant reversal in the sign of the l -(T -) doublet splittings between the particles on a sphere and the real atomic case. A systematic study of the conditional probability density

$\rho(r_1\theta_{12}|r_2=\alpha)$ for all states of a given doubly excited shell is needed to determine the full extent of the validity of the molecular picture, and work along these lines is in progress.

ACKNOWLEDGMENTS

G.S.E. would like to thank the UK Science Research Council for the award of a NATO Post-doctoral Fellowship. This work was supported in part by a grant from the National Science Foundation.

-
- ¹J. W. Cooper, U. Fano, and F. Prats, *Phys. Rev. Lett.* **10**, 518 (1963).
²C. E. Wulfman, *Phys. Lett.* **26A**, 397 (1968).
³J. S. Alper and O. Sinanoglu, *Phys. Rev.* **177**, 77 (1969).
⁴J. S. Alper, *Phys. Rev.* **177**, 86 (1969).
⁵J. Macek, *J. Phys. B* **1**, 831 (1968).
⁶C. E. Wulfman, *Chem. Phys. Lett.* **23**, 370 (1973).
⁷O. Sinanoglu and D. R. Herrick, *J. Chem. Phys.* **62**, 886 (1975).
⁸C. D. Lin, *Phys. Rev. A* **10**, 1986 (1974).
⁹U. Fano, *Phys. Today* **29:9**, 32 (1976).
¹⁰S. I. Nikitin and V. N. Ostrovsky, *J. Phys. B* **9**, 3141 (1976); **11**, 1681 (1978).
¹¹D. R. Herrick and M. E. Kellman, *Phys. Rev. A* **18**, 1770 (1978).
¹²D. R. Herrick and M. E. Kellman, *Phys. Rev. A* **21**, 418 (1980).
¹³D. R. Herrick, M. E. Kellman, and R. D. Poliak, *Phys. Rev. A* **22**, 1517 (1980).
¹⁴M. E. Kellman and D. R. Herrick, *Phys. Rev. A* **22**, 1536 (1980).
¹⁵M. E. Kellman and D. R. Herrick, *J. Phys. B* **11**, L755 (1978).
¹⁶G. Herzberg, *Molecular Spectra and Molecular Structure* (Van Nostrand, New York, 1945), Vol. II.
¹⁷A. Bohr, *Rev. Mod. Phys.* **48**, 365 (1976).
¹⁸P. Rehms, M. E. Kellman, and R. S. Berry, *Chem. Phys.* **31**, 239 (1978).
¹⁹P. Rehms and R. S. Berry, *Chem. Phys.* **38**, 257 (1979).
²⁰H.-J. Yuh, G. S. Ezra, P. Rehms, and R. S. Berry, *Phys. Rev. Lett.* **47**, 497 (1981).
²¹G. S. Ezra and R. S. Berry (unpublished).
²²D. R. Herrick, *Phys. Rev. A* **22**, 1346 (1980).
²³P. R. Bunker and J. M. R. Stone, *J. Mol. Spectrosc.* **41**, 310 (1972).
²⁴D. M. Brink and G. R. Satchler, *Angular Momentum* (Clarendon, Oxford, 1968).
²⁵J. O. Hirschfelder and E. P. Wigner, *Proc. Natl. Acad. Sci. USA* **21**, 113 (1935).
²⁶G. Breit, *Phys. Rev.* **35**, 569 (1930).
²⁷J. W. Warner, L. S. Bartell, and S. M. Blinder, *Int. J. Quant. Chem.* **18**, 921 (1980).
²⁸P. R. Bunker and D. Papousek, *J. Mol. Spectrosc.* **32**, 419 (1969).
²⁹G. Herzberg, *Molecular Spectra and Structure* (Van Nostrand, New York, 1950), Vol. I.
³⁰S. Califano, *Vibrational States* (Wiley, New York, 1976).
³¹H. Herold and H. Ruder, *J. Phys. G* **5**, 341 (1979); G. Wunner, H. Ruder, and M. Reinecke, *ibid.* **6**, 1359 (1980).
³²A. Brickstock and J. A. Pople, *Philos. Mag.* **43**, 1090 (1952).
³³R. B. Walker and R. E. Wyatt, *J. Chem. Phys.* **57**, 2728 (1972); S. H. Harms and R. E. Wyatt, *ibid.* **62**, 3162, 3173 (1975); A. B. Elkowitz and R. E. Wyatt, *ibid.* **62**, 3683 (1975); A. B. Elkowitz and R. E. Wyatt, *ibid.* **63**, 702 (1975); S. H. Harms, A. B. Elkowitz, and R. E. Wyatt, *Mol. Phys.* **31**, 177 (1976).